

# **LEGIBILITY NOTICE**

A major purpose of the Technical Information Center is to provide the broadest dissemination possible of information contained in DOE's Research and Development Reports to business, industry, the academic community, and federal, state and local governments.

Although a small portion of this report is not reproducible, it is being made available to expedite the availability of information on the research discussed herein.

OCT 09 1985

Los Alamos National Laboratory is operated by the University of California for the United States Department of Energy under contract W-7405-ENG-36

TITLE VERIFICATION OF FIRE AND EXPLOSION ACCIDENT ANALYSIS CODES (FACILITY DESIGN AND PRELIMINARY RESULTS)

AUTHOR(S) W. S. Gregory, Q-6  
B. D. Nichols, Q-6  
D. V. Talbott, Q-6  
P. R. Smith, NMSU, Las Cruces, NM 88003  
D. L. Fenton, NMSU, Las Cruces, NM 88003

LA-UR--85-3345

DE86 000811

SUBMITTED TO Commission of the European Communities  
Information Symposium on Gaseous Effluent Treatment in  
Nuclear Installations, Luxembourg, Belgium, October 14-18, 1985.

DISCLAIMER

This report was prepared as an account of work sponsored by an agency of the United States Government. Neither the United States Government nor any agency thereof, nor any of their employees, makes any warranty, express or implied, or assumes any legal liability or responsibility for the accuracy, completeness, or usefulness of any information, apparatus, product, or process disclosed, or represents that its use would not infringe privately owned rights. Reference herein to any specific commercial product, process, or service by trade name, trademark, manufacturer, or otherwise does not necessarily constitute or imply its endorsement, recommendation, or favoring by the United States Government or any agency thereof. The views and opinions of authors expressed herein do not necessarily state or reflect those of the United States Government or any agency thereof.

MASTER

By acceptance of this article, the publisher recognizes that the U.S. Government retains a nonexclusive, royalty-free license to publish or reproduce the published form of this contribution, or to allow others to do so, for U.S. Government purposes.

The Los Alamos National Laboratory requests that the publisher identify this article as work performed under the auspices of the U.S. Department of Energy.

Los Alamos Los Alamos National Laboratory  
Los Alamos, New Mexico 87545

VERIFICATION OF FIRE AND EXPLOSION ACCIDENT ANALYSIS CODES  
(Facility Design and Preliminary Results)

W. S. GREGORY, B. D. NICHOLS, and D. V. TALBOTT  
Los Alamos National Laboratory

P. R. SMITH and D. L. FENTON  
New Mexico State University

Summary

For several years, the US Nuclear Regulatory Commission has sponsored the development of methods for improving capabilities to analyze the effects of postulated accidents in nuclear facilities; the accidents of interest are those that could occur during nuclear materials handling. At the Los Alamos National Laboratory, this program has resulted in three computer codes: FIRAC, EXPAC, and TORAC. These codes are designed to predict the effects of fires, explosions, and tornados in nuclear facilities. Particular emphasis is placed on the movement of airborne radioactive material through the gaseous effluent treatment system of a nuclear installation.

The design, construction, and calibration of an experimental ventilation system to verify the fire and explosion accident analysis codes are described. The design emphasizes system characteristics and includes multiple chambers, blowers, dampers, and filters. An interconnected ductwork system that can withstand 138-kPa explosions is included, as is an apparatus to monitor accumulated aerosol mass on high-efficiency particulate air (HEPA) filters. The facility features a large industrial heater and several aerosol smoke generators that are used to simulate fires. Both injected thermal energy and aerosol mass can be controlled using this equipment. Explosions are simulated with H<sub>2</sub>/O<sub>2</sub> balloons and small explosive charges.

Experimental measurements of temperature, energy, aerosol release rates, smoke concentration, and mass accumulation on HEPA filters can be made. Volumetric flow rate and differential pressures also are monitored. The initial experiments involve varying parameters such as thermal and aerosol release rate and ventilation flow rate. FIRAC prediction results are presented.

## 1.1 Introduction

For several years, the US Nuclear Regulatory Commission has sponsored the development of methods for improving capabilities to analyze the effect of postulated accidents in nuclear facilities; the accidents of interest are those that could occur during nuclear materials handling. At the Los Alamos National Laboratory, this program has resulted in three computer codes: FIRAC, EXPAC, and TORAC. These codes are designed to predict the effects of fire, explosions, and tornados in nuclear facilities. Particular emphasis is placed on the movement of airborne radioactive material through the gaseous effluent treatment system of a nuclear installation.

At this time, there is a need to validate these codes by comparing their predictions with experimental data. We have used fire-related experimental data from the Lawrence Livermore National Laboratory (LLNL) fire test facility to compare fire compartment models. The LLNL facility is an excellent resource for investigating fire behavior in a single compartment under forced-ventilation conditions. However, it has the following limitations for meeting our needs in validating our fire, explosion, and tornado codes.

- A network ventilation system is not available.
- Multiple compartments or chambers are not available.
- Multiple dampers and blowers are not available.
- The facility is not hardened to accommodate explosive experiments.
- There is no apparatus to measure mass (smoke) accumulation on filters.

For these reasons, we have chosen to design, construct, and instrument a code verification facility that will encompass the above listed features.

In this paper we will describe the code verification facility, its instrumentation, the initial tests for fire code verification, and the FIRAC modeling and predictions for selected test parameters.

## 2.1. Facility Description

The multicompartiment ventilation system model is installed inside a prestressed concrete building that provides environmental control. The building is located at the Mechanical Engineering Test Site, which is on the campus of New Mexico State University. The model ventilation system is designed to accommodate thermal, pressure, and aerosol inputs. The thermal inputs are generated by a commercially available duct heater rated at 92 000 kcal/h fired by natural gas and limited to a maximum of 300°C. The duct heater is on casters, permitting thermal inputs at different locations of the model system. Pressure pulses are limited to a 140-kPa overpressure and must originate in the rectangular volume. A mechanical safety factor of 3 characterizes the design of the pipe and square ducts. The particulate mass input is provided by a commercial dust reader capable of supply rates varying between 1 and 40 g/min (particulate material density = 1 g/cm<sup>3</sup>). The maximum particulate mass concentration is approximately 1.4 g/m<sup>3</sup> for unit density particulate material.

The model ventilation system's arrangement of ducts and volumes is shown in Fig. 1. For economy, 30.5-cm-diam Schedule 20 pipe is used for the bypass loop around the two volumes and the connections between the two volumes. The 0.6-m-square ducts were fabricated from 0.64-cm steel plate and are used for the remainder of the ventilation system; the system's straight length is approximately 24.4 m. The inlet and outlet round duct connections occur within the lower third of the rectangular tank and differ by 0.69 m vertically. Figure 1 shows one circular duct connecting to

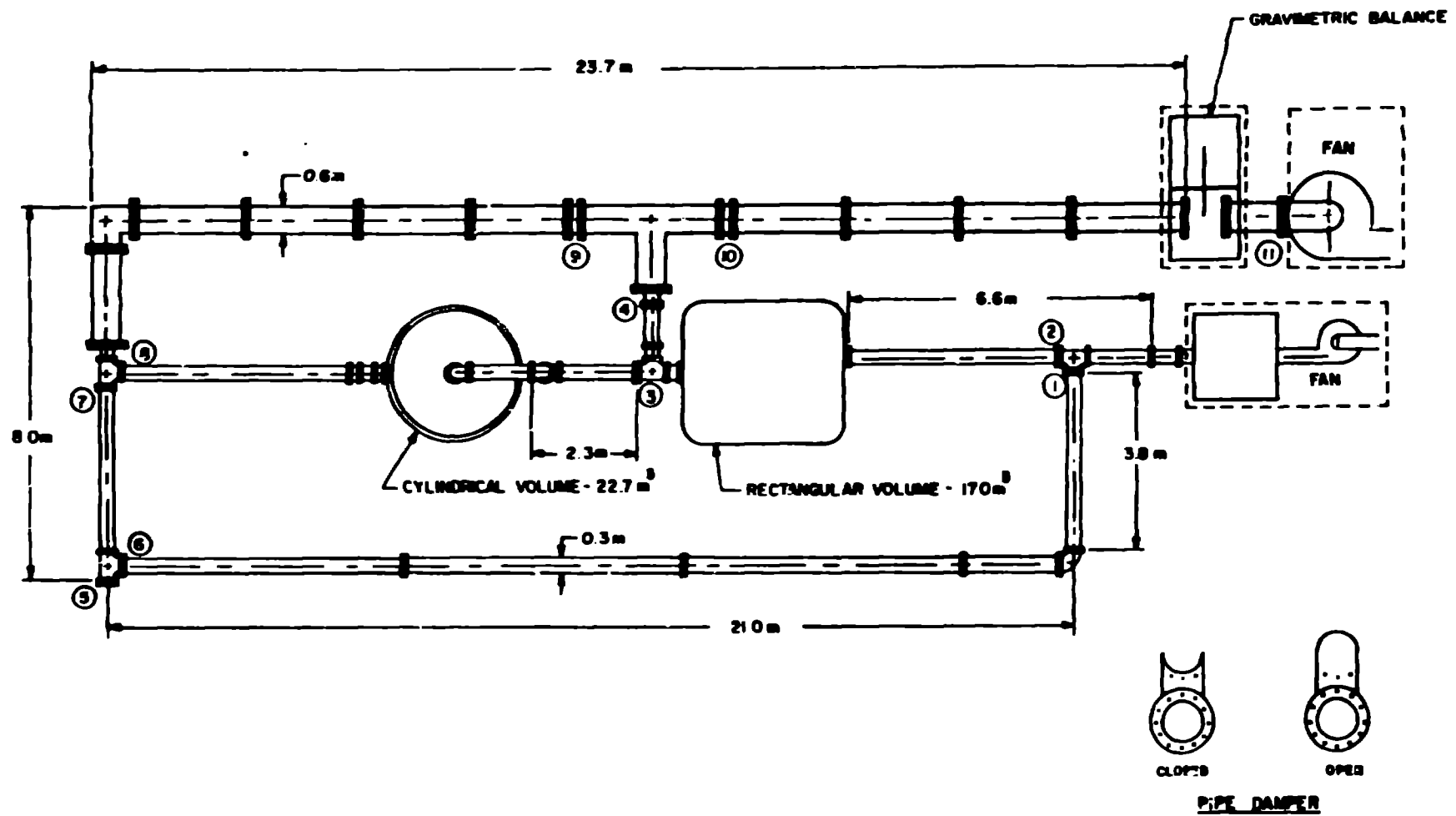


Fig. 1. Schematic of the code verification apparatus.

the top of the cylindrical volume and the other circular duct connecting to the side of the volume (lowest possible location). The centerline distance of both the round and square ducts above the floor is 1.7 m.

The two volumes are essentially steel tanks modified as shown in Fig. 1. The rectangular tank (17.0 m<sup>3</sup>) has 5-cm-thick walls and can withstand the largest pressure pulses. The remainder of the system limits the maximum pressure pulse to about 140 kPa over-pressure. The cylindrical tank (22.6 m<sup>3</sup>) is upright to provide the maximum possible stratification and serves as a location for thermal and/or particulate mass input. The cylindrical tank is 4.6 m high. The two fans included in the facility provide positive or negative pressures within the model ventilation system.

The round duct dampers are numbered in Fig. 1 and are reversible 1.27-cm steel plates that are secured by the pipe flanges. These dampers are either full open or closed. Additionally, three dampers are located in the square duct between the HEPA filter gravimetric balance and fan, upstream from the square duct tee, and downstream from the square duct tee. Dampers 9 and 10 are commercial and thus adjustable, but damper 11 is conceptually similar to the round duct dampers. Numerous model system configurations are possible by opening and closing the dampers. The HEPA filter gravimetric balance is specially designed to measure the collected mass on a HEPA filter installed in the system. The balance uses a null technique and an electronic force transducer to achieve a resolution of 2 g.

This model ventilation system is three-dimensional because of the vertical height associated with the cylindrical volume. Thus, thermal loads or "test fires" (possibly in conjunction with a particulate mass) can be input to the base of the cylindrical volume, and the transport of both thermal energy and particulate material can be observed in the model ventilation system. Additionally, the gravimetric balance can determine the collected particulate mass on the HEPA filter. Careful collection of particulate material on the internal surfaces yields information on total deposition.

FIRAC code verification involves instrumentation that measures the following experimental variables.

1. Temperature [ambient air inlet (dry and wet bulb), upstream from HEPA filter, downstream from HEPA filter]
2. Particulate mass concentration (aerosol source and upstream from HEPA filter)
3. Volumetric airflow rate (HEPA filter)
4. Pressure drop (across HEPA filter)
5. Particulate mass (accumulated on HEPA filter)
6. Particulate mass deposition (selected locations)

Instrumentation for the pressure pulse tests would include most of the above measurements (depending on the specific test objectives) but always would include transient pressure measurements to characterize the attenuation of the shock waves initiated by the pulse.

### 3.1 FIRAC Modeling

The FIRAC computer code initially was designed to predict fire-induced transients in nuclear fuel cycle facility ventilation systems. FIRAC simultaneously calculates the gas dynamic, material transport, and heat transport transients that occur in any arbitrarily connected network system subjected to a fire. The network system includes ventilation system components such as filters, dampers, ducts, and blowers. These components are connected to the rooms and corridors to complete the network for moving air through the facility.

We use the lumped-parameter method to describe the airflow system. No spatial distribution of parameters within the network components is included in this approach. Network theory defines system elements that exhibit flow resistance and inertia, or flow potential, as branches. Ventilation system components contained in branches include dampers, ducts, valves, filters, and blowers. The connecting points of branches are network system elements called nodes and always have a finite volume. Nodes include specific network components that have finite volumes, such as rooms, gloveboxes, and plenums, or the node may contain only the volume of the connecting branches. In addition, system boundaries where the volume is practically infinite are specified as nodes. Fluid mass and energy storage at the internal nodes is taken into account by using the equations for conservation of mass and energy. The conservation equations are applied to the room nodes using the lumped-parameter formulation assuming a homogeneous mixture and a thermodynamic equilibrium. An implicit numerical scheme is used to solve for the pressure and density at each node. In the solution algorithm, the flow rate through branches is modeled as a function of the differential pressure and friction factors.

The material transport model in the code estimates the movement of material through the network of ventilation system components. The code calculates material concentrations and material mass flow rates at any location in the network. This model includes convective transport, depletion by gravitational settling, entrainment from ducts, and filtration. No phase transitions or chemical reactions are allowed.

The heat transfer model in the code predicts how the combustion gas in the system cools as it flows through the network ducts. The model predicts the temperature of the gas leaving any section of the duct if the inlet temperature and gas properties are known. The heat transfer processes modeled are the following.

- Forced convection between the gas and the inside duct walls
- Radiation between the gas and the side duct wall
- Heat conduction through the duct wall
- Natural convection from the outside duct wall to the surrounding air
- Radiation from the outside duct wall to the atmosphere

The schematic for the verification apparatus is shown in Fig. 1. For the initial tests, we are modeling the 0.6-m by 0.6-m duct and a portion of the adjacent 0.3-m-diam pipe. Specifically, our model consists of an indirectly fired heater and a dust generator feeding into a 5-m segment of pipe that is 0.3 m in diameter with tee joints and the 28-m section of 0.6-m by 0.6-m duct with tee joints, a 90° bend, dampers, valves, a filter, and an exhaust blower. The network system model is shown in Fig. 2. The model consists of 22 nodes, including 2 boundary nodes, and 21 branches. We divided the pipe into 4 branches and the duct into 12 branches [typically 2.44-m (8-ft) segments]. We modeled each tee joint and bend as a separate branch because this allows an accurate determination of the resistance coefficients for these branches. The heater is simulated by a temperature-time history, and the dust generator is simulated by a particulate rate time history defined at Node 2.

#### 4.1 Predictive Results

We chose two sets of initial conditions to input into the verification facility apparatus model described above. In each of these, the volumetric flow rate through the system is initially  $0.236 \text{ m}^3/\text{s}$ , and the simulation continues for 300 s. In the first case, the heater input is simulated by linearly increasing the temperature in Node 2 from ambient at

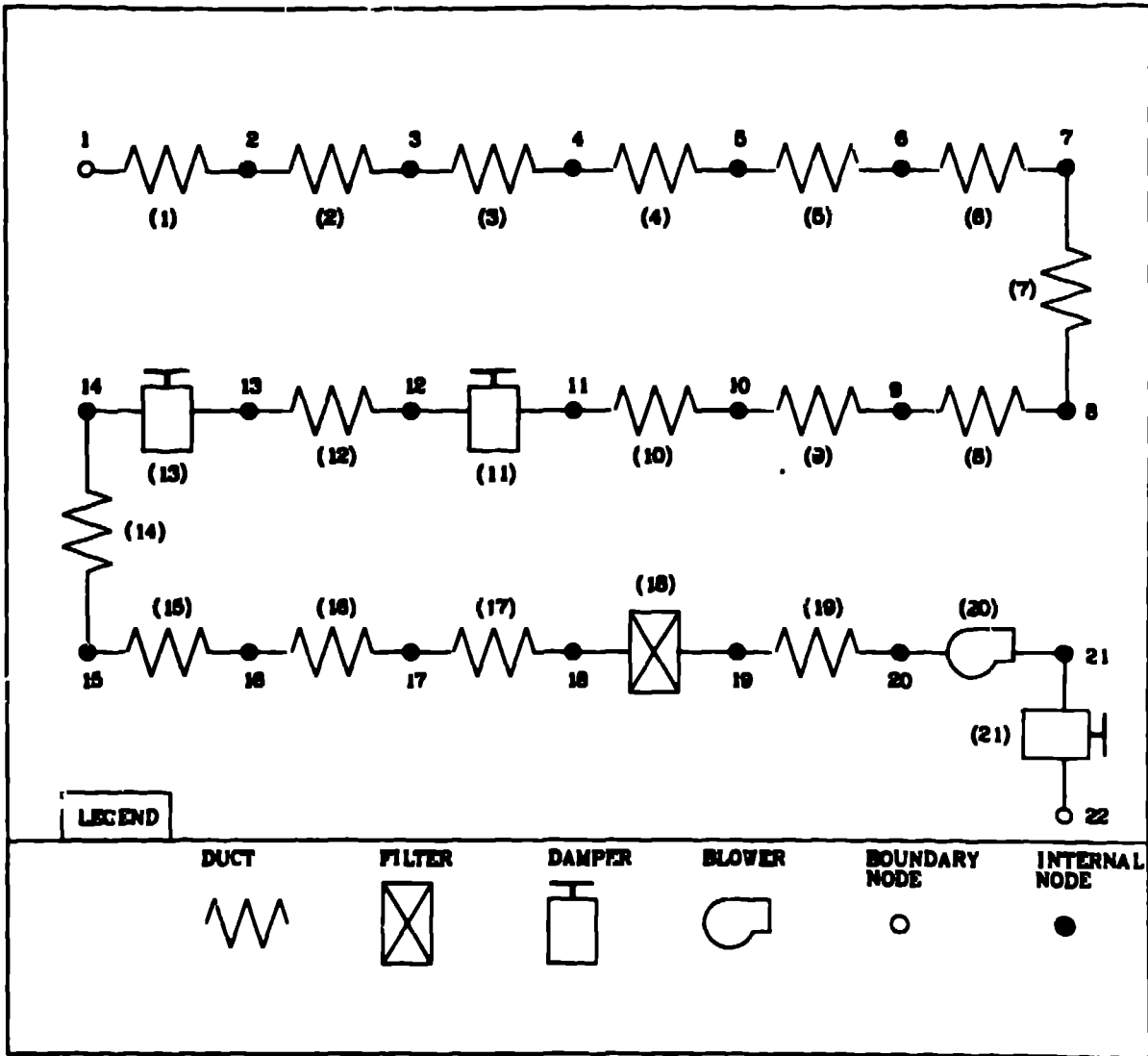


Fig. 2. Modeling schematic of the code verification apparatus.

15.6°C to 300°C over a time interval of 0 to 60 s. This simulation includes the heat transfer model, but no particulate material is included. The second case, a particulate material, 11- $\mu\text{m}$  glass spheres, is injected into the system at the rate of  $0.1333 \times 10^3 \text{ kg/s}$  that gives an initial concentration of  $0.565 \times 10^{-3} \text{ kg/m}^{-3}$ . The system is at ambient temperature.

The FIRAC output is given in tabular and graphic form. Selected plots of the results from the first case are shown in Figs. 3--6. As shown in Fig. 3, the temperature in Node 2 rises to 300°C and remains constant. The nodes farther downstream (Nodes 11, 18, and 19) are progressively lower in temperature as heat is lost from the duct. Nodes 18 and 19, which bracket the filter in Branch 18, are virtually the same because heat loss from the filter housing is not calculated.

The pressure-time histories for selected nodes are shown in Fig. 4. The negative gauge pressures are caused by the exhaust blower. The pressures in each node increase when the air is heated initially. As the duct wall temperature increases, the heat loss becomes greater than the heat gain from the incoming heated air, and the pressure drops. After 150 s, the heat addition and loss are in equilibrium, and the pressure remains nearly constant in each node.

The volumetric flow rate is governed by the exhaust blower. In Fig. 5, the volumetric flow rate is almost a steady  $0.236 \text{ m}^3/\text{s}$  in Nodes 18 and 19 because they are near the blower. The effect of heated gas is seen in Nodes 2 and 11, where the volumetric flow rate increases for the less dense gas. In Fig. 6, the corresponding effect of the heated gas on the mass flow rate is seen for Nodes 2 and 11. Here, the less dense gas has a decreased mass flow rate. As expected, the constant volume flow rates in Nodes 18 and 19 show a decreased mass flow rate as the gas temperature increases.

Selected plots of the second simulation are shown in Figs. 7--10. Particulate material is injected into the system model in Node 2 (Fig. 2) at  $0.1333 \times 10^3 \text{ kg/s}$ . The system remains at a constant temperature of 15.6°C and has an initial flow rate of  $0.236 \text{ m}^3/\text{s}$ . The particulate flow rate as a function of time for the 11- $\mu\text{m}$  glass spheres is shown in Fig. 7 for Branches 2, 10, 17 and 19. The rate of injection has reached its maximum by 70 s as is seen in the plot of the Branch 2 data. The branches farther downstream show a lower particulate flow rate because of deposition (Fig. 8) and filter plugging, which reduces the maximum flow rate through the system. (A plot is not presented, but the filter plugging is reflected by a decrease in the gas flow rate also.) Branch 19, which is downstream of the filter, shows virtually no particulate flow because the particles are stopped by the filter. The dotted line in Fig. 9 shows the increase of the particulate mass on the filter as a function of time. In addition, the particulate mass flow through Branches 2, 10, and 19 is plotted. Deposition from gravitational settling in the duct work is plotted in Fig. 10. The branches closer to the source have more material deposited than those downstream because of the decrease in material concentration downstream as the material is deposited. There is no entrainment of the glass spheres because this flow speed is below the threshold friction speed for 11- $\mu\text{m}$  spheres.

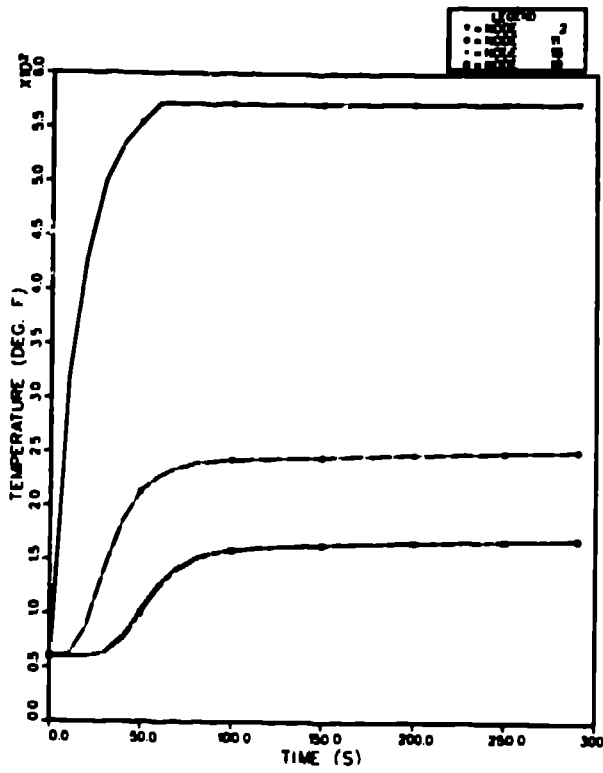
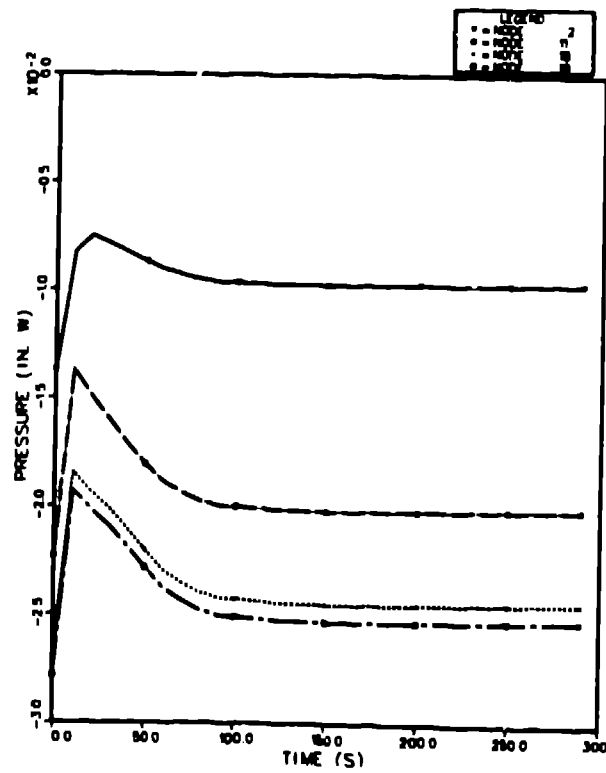


Fig. 3. FIRAC-calculated temperature time history for the sample problem.

Fig. 4. FIRAC-calculated pressure time history for the sample problem.



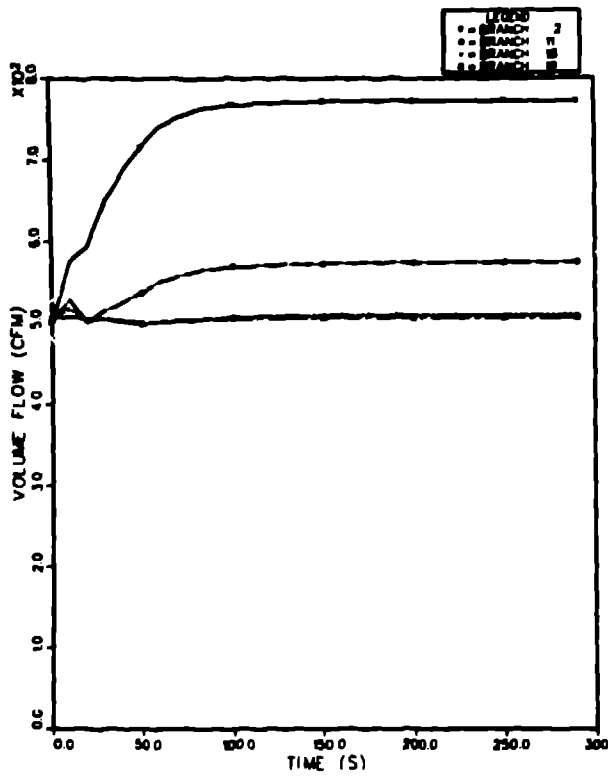


Fig. 5. FIRAC-calculated volume flow for the sample problem.

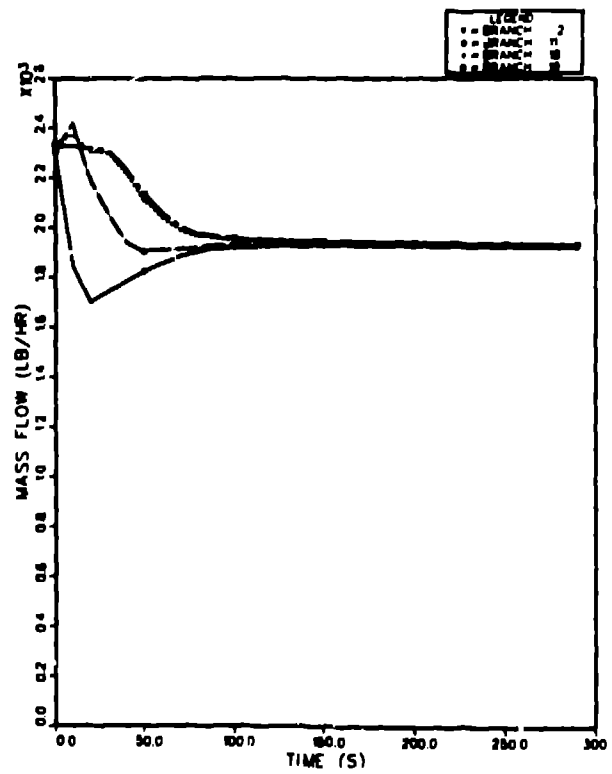


Fig. 6. FIRAC-calculated mass flow for the sample problem.

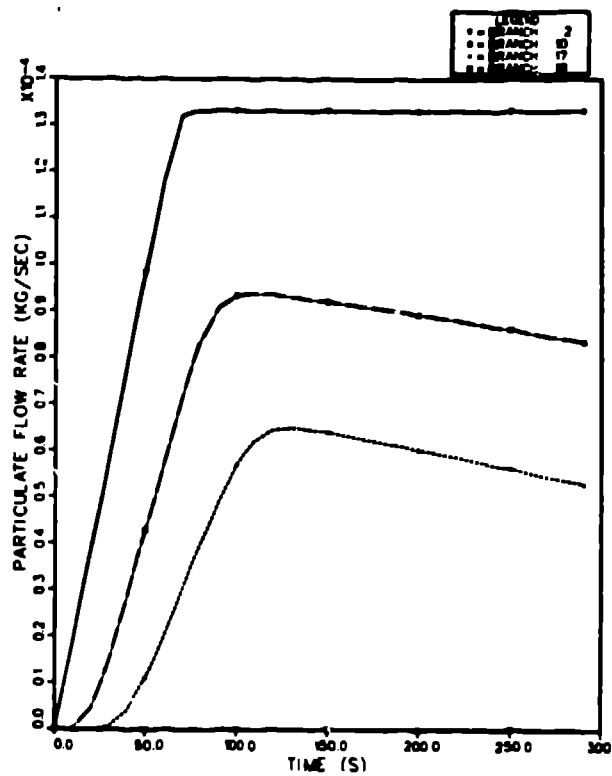


Fig. 7. FIRAC-calculated particulate flow rate for the sample problem.

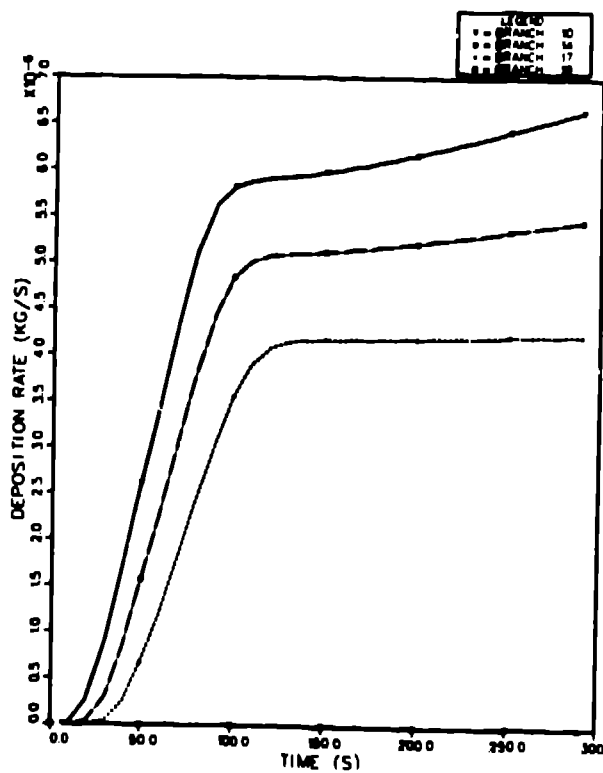


Fig. 8. FIRAC-calculated deposition rate for the sample problem.

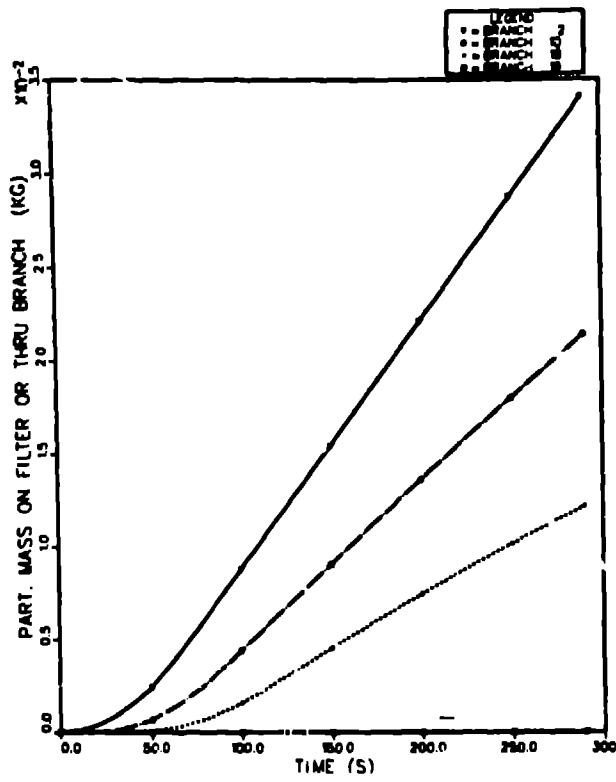


Fig. 9. FIRAC-calculated accumulation of particulate mass deposited on the filter for the sample problem.

Fig. 10. FIRAC-calculation of particulate mass deposited in the duct for the sample problem.

